



Design and Selection of High Reliability Converters for Mission Critical Industrial Applications: A Rolling Mill Case Study

A. F. Cupertino, V. N. Ferreira, H. A. Pereira, S. I. Seleme Jr. A.V. Rocha and B. J. C. Filho

Published in:

IEEE-Transactions on Industry Applications

DOI (*link to publication from Publisher*):

[10.1109/TIA.2018.2829104](https://doi.org/10.1109/TIA.2018.2829104)

Publication year:

2018

Document Version:

Accepted author manuscript, peer reviewed version

Citation for published version:

A. F. Cupertino, V. N. Ferreira, H. A. Pereira, S. I. S. Junior, A.V. Rocha and B.J. C.Filho, "Desing and selection of High reliability Converters for Mission Critical Industrial Applications: A Rolling Mill Case Study," IEEE-Transactions on Industry Application, vol. 54, no. 5, pp. 4938-4947, April 2018.
doi: 10.1109/TIA.2018.2829104

General rights

Copyright and moral rights for the publications made accessible in the public portal are retained by the authors and/or other copyright owners and it is a condition of accessing publications that users recognise and abide by the legal requirements associated with these rights.

- Users may download and print one copy of any publication from the public portal for the purpose of private study or research.
- You may not further distribute the material or use it for any profit-making activity or commercial gain
- You may freely distribute the URL identifying the publication in the public portal

Take down policy

If you believe that this document breaches copyright please contact us at gesepufv@gmail.com providing details, and we will remove access to the work immediately and investigate your claim.

Design and Selection of High Reliability Converters for Mission Critical Industrial Applications: A Rolling Mill Case Study

Victor de Nazareth Ferreira*, Allan Fagner Cupertino*[†], Heverton Augusto Pereira[‡], Anderson Vagner Rocha[†], Seleme Isaac Seleme Junior* and Braz de Jesus Cardoso Filho*

*Graduate Program in Electrical Engineering - Federal University of Minas Gerais
Av. Antônio Carlos 6627, 31270-901, Belo Horizonte, MG, Brazil
Emails: vnferreira89@gmail.com, seleme@cpdee.ufmg.br, braz.cardoso@ieee.org

[†]Federal Center for Technological Education of Minas Gerais
Av. Amazonas 5253, 30421-169, Belo Horizonte, MG, Brazil
Emails: afcupertino@ieee.org, andersonrocha@des.cefetmg.br

[‡]Department of Electrical Engineering - Federal University of Viçosa
Av. P.H. Rolfs, 36570-901, Viçosa, MG, Brazil
Emails: heverton.pereira@ufv.br

Abstract—In metals industry, rolling is the most widely used steel forming process to provide high production and control of final product. Rolling mills must be able to change the speed of the strip at the same time that the speed is controlled within precise limits. Furthermore, this application has a severe load profile, with high torque variations during the lamination process. These characteristics include rolling mills among the classical Mission Critical Industry Applications (MCIA). In addition to the high cost/failure rate, rolling mills have a critical dynamic loading, making the design of a reliable system doubly challenging. Design For Reliability (DFR) is the process conducted during the design of a component or system that ensures them to perform at the required reliability level. In the context of the power converters for rolling mills and other MCIA, the DFR should be known and adopted in the design of the converter proper (component level) well as in the specification of power converters (system level). This paper contributes to the knowledge in the field by proposing a methodology covering the necessary steps for decision-making during the design (component level) and selection (systems level) of power converters for MCIA. A rolling mill system from a large steel plant in southeastern Brazil is adopted as case study. The standard high power converter solution is compared with two high reliability converter topologies: the FT-ANPC and the TSBC-MMC. The importance of DFR in mission critical applications is demonstrated.

I. INTRODUCTION

The term Mission Critical Industry Application (MCIA) refers to any application that is required by important industrial processes to run. In MCIA, a single failure may lead to higher than the overall system cost, including parts replacement, travelling of maintenance personnel, and penalty charges [1].

Steel is nowadays the world's most important industrial material, with over 1.5 billion tons produced annually. In metals industry, rolling is the most widely used steel forming process to provide high production and control of final product.

Rolling mills must be able to change the speed of the strip at the same time that the speed is controlled within precise limits [2]. Furthermore, this application has a severe load profile, with high torque variations during the lamination process. These characteristics include rolling mills among the classical MCIA.

AC medium-voltage (MV) power converters play a vital role to meet many demands of the modern steel industry. In the MW range, medium-voltage drives are preferred due to their higher efficiency and higher power density [3]–[5]. The importance of these converters in critical industrial processes culminated in extraordinarily high availability requirements. For about 30 years, the three-level neutral-point-clamped voltage-source (3L NPC VSC) converter has been the standard solution in the medium-voltage range for industrial applications [6]. Nevertheless, the NPC converter has an inherent problem in the distribution of losses between phase switches, which can reduce its power capacity and compromise the semiconductors reliability [7], [8].

The main problem with the application of off-the-shelf converter solutions in MCIA is the inherent lack of fault tolerance, which means that the system operation is interrupted under any failure situation. A typical solution is the addition of a backup converter, although fault tolerant topologies would lead to lower cost solutions and to the capacity to survive multiple failures.

In addition to the high cost/failure rate, rolling mills have a critical dynamic loading, making the design of a reliability system doubly challenging. Design For Reliability (DFR) is the process conducted during the design procedure of a component or system that ensures them to perform at the required reliability level. It aims at identifying and fixing the weak links up-front, in the design stage [10]. In the context

of the power converters, the DFR should then be known and adopted in the design of the converter proper (component level) well as in the specification of the process components (system level). At system level and in the context of this paper, DFR implies proper evaluation and selection of power converters, aiming to achieve the required reliability.

In the literature, several methodologies have been proposed to compare and select topologies for a given application. Reference [9] presents a comparison of 3 multilevel topologies for STATCOM applications. In [10], it is discussed the design and control of two converter topologies for grid connected applications. Energy storage systems are discussed in [11], where many voltage classes of power semiconductors are employed. In these references, power losses, efficiency and cost are evaluated but no attention is given to reliability.

Some research work has been directed to the reliability of power converters for given mission profiles. For instance, photovoltaic systems have been studied in [12]–[15], while wind energy systems have been approached in references [16]–[19]. Smart-transformers have been discussed in [20]–[22]. However, these research works do not propose the adoption of reliability as a figure of merit to compare and rank power converter topologies. In this sense, a reliability analysis and design for a mine hoist system is presented in [23], but there is no discussion on costs or on overall power losses during the converter operation. This is an interesting work addressing the converter design for reliability (component level) but no methodology is presented for decision making at systems level.

This paper contributes to the knowledge in the field by proposing a methodology covering the necessary steps for decision-making during the design (component level) and selection (systems level) of power converters for MCIA. A rolling mill system from a large steel plant in southeastern Brazil is adopted as case study. Two high reliability converter topologies are compared with the off-the-shelf solution: the FT-ANPC [24] and the TSBC-MMC [25]–[27]. Also an original contribution, it is presented the reliability analysis of the recently proposed TSBC-MMC topology along with its comparison with already existing high power converter topologies.

The outline of this paper is as follows. Section II introduces a methodology for evaluation and selection of high reliability power converters. In section III, it is developed a case study to illustrate the proposed methodology based on data from an existing rolling mill. A decision-making procedure is discussed in section IV. Finally, the conclusions are stated in Section V. This paper is a reviewed and extended version of a recently presented conference paper [28].

II. DESIGN AND SELECTION OF HIGH RELIABILITY CONVERTERS

The design and selection of high reliability converters for MCIA is challenging, often requiring multidisciplinary analysis. Many factors contribute to this scenario: efficiency, power density, cost and reliability. The flowchart shown in

Figure 1 presents the evaluation and selection methodology considered in this work. It can be noticed that the proposed methodology is based on the DFR process, a very interesting way when critical applications are taken into account. [23].

The first step in the evaluation process is the mission profile definition for the considered application. Basically, this information is necessary to estimate the operational conditions of the power converter. This mission profile must be as close as possible to the real operational conditions. If possible, measurements can be performed. The mission profile fidelity will affect the quality of the analysis.

The next step is the power converter selection. Depending on the voltage and current values, the most appropriate power converter can be selected. Using the mission profile, the passive components of the converter can be designed. Additionally, the mission profile is used to define the power rating and the overload capacity of the power converter.

When the topology is chosen, a simulation model can be used to estimate the current and voltage waveforms synthesized by the converter. Initially, the power semiconductors are chosen considering their current and voltage ratings. Nevertheless, this selection cannot be suitable depending of the reliability requirements. Therefore, the DFR approach is employed in this step.

Basically, the converter power losses are estimated using the current and voltage waveforms and the technical data of the power semiconductors. The main goal in this step is to estimate the junction and case temperatures in the power modules. The conduction and switching losses are estimated through look-up tables based on the data provided in datasheets [29]. After that, the junction and case temperatures of the power devices are also estimated, considering the thermal model proposed in [30]. As observed, this process is dynamic, since the temperature and power losses are coupled.

The next step is to estimate and analyze power losses are estimated and can be analyzed. Furthermore, the junction and case temperatures are obtained. In this step, a cycle counting must be used to characterize the thermal cycling in the power devices [13]. Using these data, a lifetime model can be employed to predict the lifetime consumption with a given confidence interval. If the lifetime is not sufficient for the application, other power module must be selected. Generally, power modules with larger current capability or parallel connections are considered in this step.

When the required lifetime is reached, the cost and energy losses are evaluated. If the cost is unacceptable, other topology must be selected. In this case, all the steps previously discussed must be repeated.

III. CASE STUDY

In order to exemplify the proposed methodology, a real case of 7 MW rolling mill system installed in the southeastern Brazil is approached. Following the procedure, the field and design engineers will be capable to design or select a high reliability converter for its application. The schematic of the rolling mill diagram is shown in Figure 2. As observed,

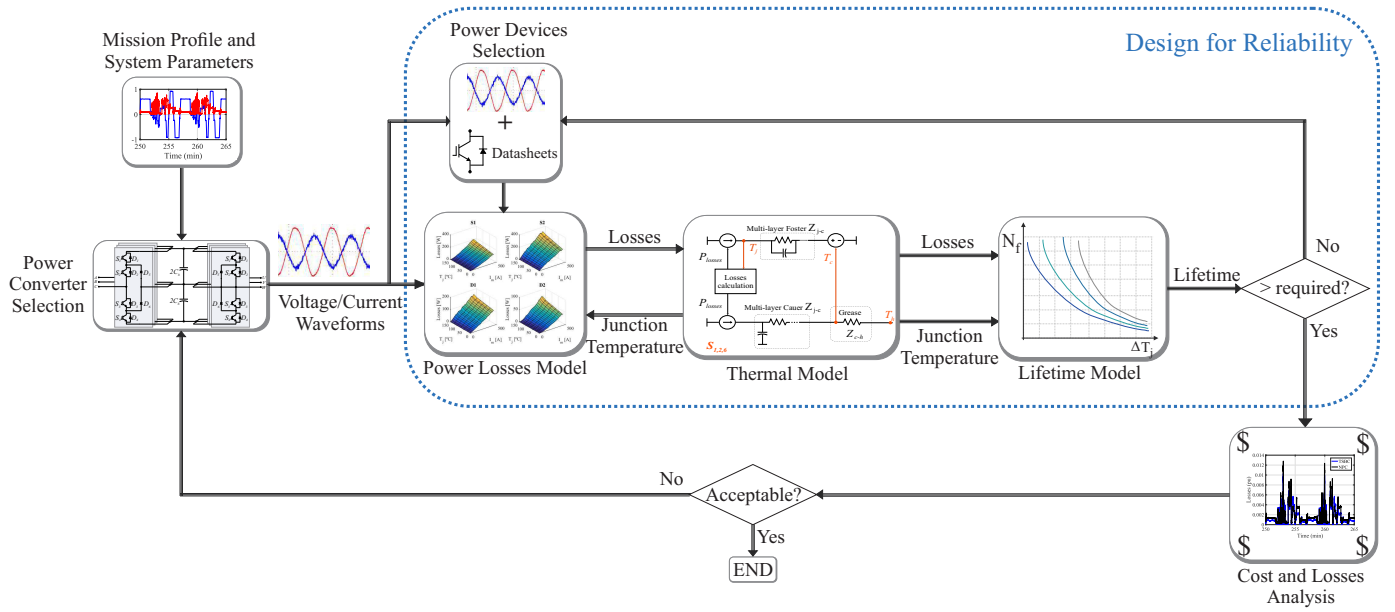


Fig. 1. Methodology for evaluation and selection of high reliability converters for critical applications.

this system is based on a dual stator winding synchronous machine, which parameters are reported in Table I. The overload capability can reach 250% for 20 seconds. The standard solution is based on the traditional NPC converter. For sake of clarity, the study is based in one side of stator winding, for the other side we can consider the same structure.

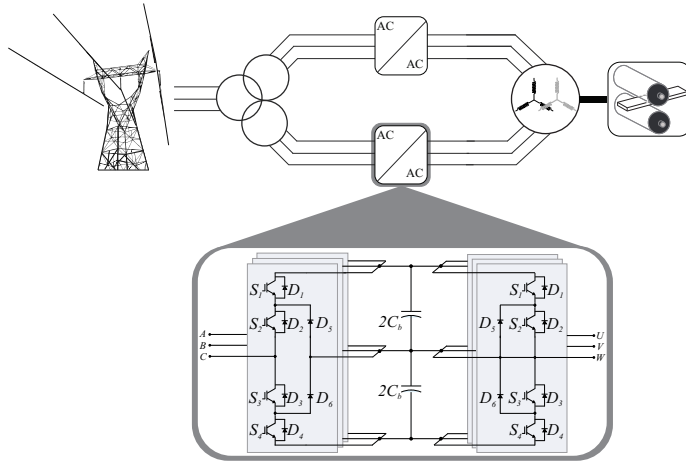


Fig. 2. Schematic for the mill system located in the southeastern Brazil with the standard solution.

A. Mission Profile

The mission profile of the rolling mill system is analyzed over a full day operation, 8 hours of functionality with three stops and about of 60 laminated parts. The mechanical speed n_m and the stator current (rms) I_s were obtained from field measurements. The sampling frequency of the data is 100 ms. The per-unit (pu) values¹ are presented in Figure 3. As clearly

¹Bases: 255 min^{-1} for mechanical speed and 1815 A for stator current.

TABLE I
RATINGS FOR THE DUAL WINDING SYNCHRONOUS MACHINE EMPLOYED IN THE ROLLING MILL SYSTEM.

Operating Data	Rated Point	Max. Cont.	Peak (20 s)
Output (MW)	7	8	17.5
Line Voltage (V)	3150	3150	3150
Frequency (Hz)	8.5	8.5	25.5
Line Current (A)	667A	774	1815
Power Factor	0.99	0.99	1
Speed (min^{-1})	85	85	255

observed, this application has a really critical load cycling, with a notable electrical current variation all day long.

Regarding to the power losses modeling, the electrical currents as well as the output voltages synthesized by the converter are necessary. The converter voltage is estimated through the mechanical speed. Basically the machine frequency is obtained using the machine pole number information. Following, a scalar control strategy (V/Hz) with field weakening operation is assumed. Therefore, the voltage is proportional to the frequency until the rated point. In the field weakening region, the voltage is maintained constant and the frequency increases.

B. Power Converter Selection

In this section two high reliability topologies that can be chosen for MV rolling mill system are presented. The first one is the FT-ANPC converter, which has been shown to be very promising for high-power mission critical applications [23] [31]. The second one is the Triple-Star Bridge Cells Modular Multilevel Converter (TSBC-MMC), which is emerging as a promising high reliability solution for electrical drives with high torque requirements at low speeds [27], [32]. The main

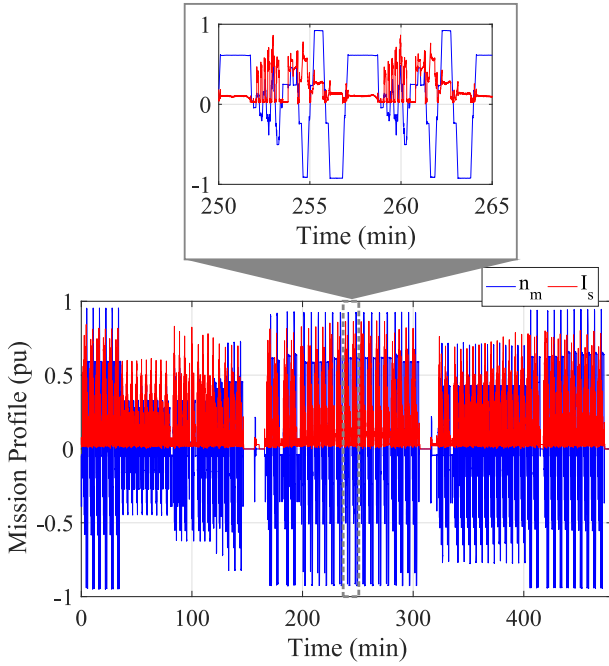


Fig. 3. Mission profile for the rolling mill system.

features of these topologies are detailed, highlighting their fault tolerance capability and control strategies.

1) *Fault-tolerant ANPC*: In 2001, the 3L Active Neutral Point Clamped (ANPC) converter was introduced to overcome the main structural drawback of the 3L-NPC VSC, regarding the power losses distribution [33]. The proposed topology employs two extra active switches per phase compared to the original NPC structure (Figure 4). The additional active switches add new commutation modes, allowing substantial improvement of the loss distribution among the converter power devices [7], [8]. As a result, the output power can be increased by up to 25%, keeping the switching frequency, by using 3L-ANPC VSC [8].

The FT-ANPC concept is based on the premise that the ANPC structure can be designed aiming to overcome failure situations extending the converter lifetime. These benefits are achieved by adding minimal extra parts and using existing connections in the commercial well known ANPC converter [24]. As can be seen in Figure 4, two IGBTs (S_5 and S_8) with their respective free-wheeling diodes (D_5 and D_8) are added per phase. Also, a switch (K_c) with two reversible contacts is introduced. The K_c is not a critical device since it is commutated under zero current, and can be implemented with simple contactors or manual operated switches. With these extra components, the new topology of neutral point clamped converter is capable of changing its configuration in multiple ways.

Phase legs L_1 and L_2 can operate in two different complementary modes through K_c : Phase (P) and Neutral (N). For example, if L_1 is connected to the neutral point (N), L_2 is necessarily connected to the phase point (P), and

vice-versa. Since this converter operates as a NPC or ANPC, some simple reconfigurations can also be made. The external devices of the right leg (S_1 and S_4) can be interchanged with the external devices of the right leg (S_5 and S_8) by software. To interchange the internal devices (S_2/S_3 and S_6/S_7), it is necessary to stop the converter switching allowing the current to go to zero. Thus, K_c can be switched, changing the connection of L_1 and L_2 . From its reconfiguration capabilities, the FT-ANPC converter has been shown to be able to prolong considerably the power devices lifetime, and to survive up to four consecutive failure situations in one phase, without compromising the load operation, before to shutdown the converter. Figure 4 shows a back-to-back structure composed by two FT-ANPC converters.

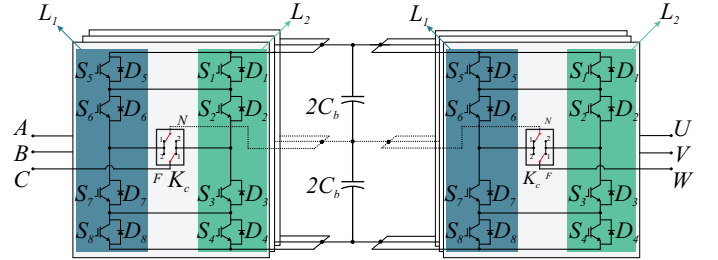


Fig. 4. Schematic of back-to-back fault-tolerant ANPC converter.

Regarding the control of FT-ANPC topology, the three-level space vector pulse width modulation (SVPWM) [34] and the ANPC feedforward loss control [35] are used to obtain the required output voltage and improve the losses distribution.

The vector control of the induction motor speed is implemented according to reference [36]. The inner loops are implemented in synchronous (dq) reference frame oriented in rotor flux, resulting in a decoupled control of magnetization flux and torque. The external loops control the motor speed ω^* and the magnetization flux λ_m . This control strategy calculates the output voltage reference.

The three-phase ac/dc stage control is based on a cascade strategy, as described in [37]. The internal loops regulates the grid currents while the outer control loop regulates the dc-link voltage and the reactive power injected in the main grid. During the braking process, the rectifier is responsible to inject the energy back the grid.

The dc-link of the FT-ANPC converter selected for this case study is composed by 12 Al-Caps of 2800V and 2 mF, totaling 6 mF of equivalent capacitance.

2) *TSBC-MMC*: The modular multilevel converters (MMC) family is considered an emerging high power converters for medium voltage drives. The MMC concept is to obtain a high voltage converter using a cascade connection of low voltage units, called cells or submodules (SMs). The first MMC topology discussed in literature for medium voltage drives is based on the double-star chopper cells modular multilevel converter (DSCC-MMC). However, this topology presents some limitations in low speed region. Basically, when the converter synthesizes low frequencies, the voltage ripples

across the SM capacitors increase considerably. Additionally, higher values of circulating current are necessary to obtain rated torque at standstill. Although some solutions have been proposed to improve the performance of this topology, the DSCC-MMC is not considered a suitable topology for rolling mills applications, where large values of torque are necessary in a very low speed region [25].

For rolling mills application, the triple-star bridge cells MMC (TSBC-MMC) is more suitable, as discussed in [25]–[27]. This topology does not present an increase in voltage ripple or circulating currents in low frequency region. The schematic of TSBC-MMC is presented in Figure 5. As observed, TSBC-MMC presents 9 clusters and enables direct three phase ac-to-ac bidirectional power conversion with any power factors at both sides [32]. This topology is also known as Modular Multilevel Matrix Converter [27].

Each SM contains a capacitance C and eight semiconductor switches ($S_1, S_2, S_3, S_4, D_1, D_2, D_3$ and D_4). The cluster inductance L is responsible for reducing the high order harmonics in the circulating current and also limiting the currents during faults [38]. The converter presents N SM per cluster. Generally, there is a switch S_T in parallel with each SM, which is responsible for bypassing it in case of failures [39].

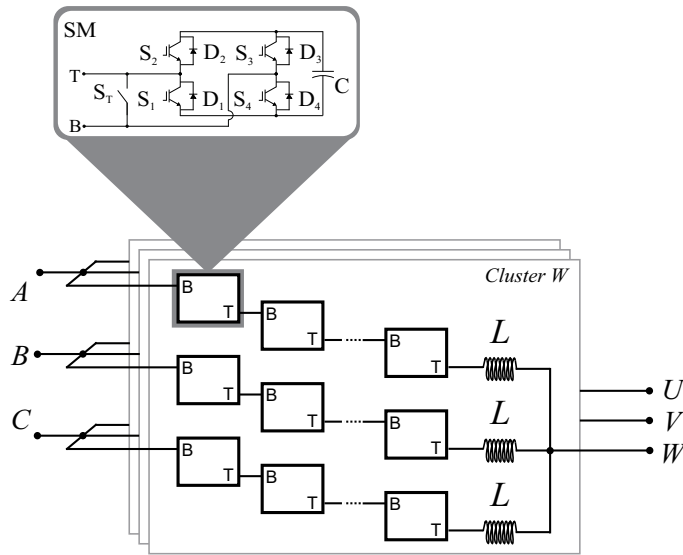


Fig. 5. Schematic of the TSBC-MMC converter.

The TSBC-MMC topology is often featured with its robustness in terms of SM failures. When power switch failures are identified (generally by advanced gate drives), the corresponding SM should be bypassed [40]. In order to ensure that the converter remains operational during failures, some redundancy strategy needs to be included to the converter structure [41]. Therefore, the operation of the converter can continue without affecting the overall performance [42]. This condition is attended for a percent number of SM failures. In most works in literature, the redundancy factor is something

around 10 % [43]. It means that the operation of the converter can continue until the failure of 10 % of SMs.

In [44] the MMC redundancy strategies are classified into two schemes: hot reserve and cold reserve. In hot reserve based strategies the redundant SMs operate in the same way as other SMs. When a fault occurs, the faulty SM is bypassed while the MMC keeps working correctly [44], [45]. In cold reserve based strategies the redundant SMs are bypassed and discharged. When a fault occurs, the corresponding faulty SM is bypassed and the redundant SM is inserted into the main circuit [44], [45]. Thereby, the hot reserve based strategies can lead to asymmetrical operation in the converter and larger power losses, while the cold reserve based strategies presents more significant transients during failures.

Regarding the control strategy of the TSBC-MMC, it can be divided in four main functions: Motor control, mean voltage control, circulating current control and capacitor balancing control [46].

The vector control of the induction motor speed following the same approach described by FT-ANPC converter. The mean voltage control structure is similar to the control of NPC ac/dc converter. This loop is responsible for determining the amount of active power which flows to the converter. The reactive power is also controlled, resulting in a full control of the grid current power factor. Inner loops in synchronous reference frame regulates the grid currents

The capacitor balancing control regulates the voltages in all capacitors of the converter. These loops calculates the value of the circulating currents (four circulating currents can be identified), which will result in power exchange between the clusters. By using the circulating currents, it is possible to exchange power between the clusters without affect the input or output currents. Phase-shifted pulse-width modulation is employed. More details about the control strategy can be found in references [26], [27].

The TSBC-MMC does not have a dc-link due to its direct ac-ac conversion. Nevertheless, the sub-module capacitor bank design is a critical point for this topology, since there is a high ac circulating current. The selected topology for this application presents 6 SMs per cluster. Therefore, the nominal voltage in each SM is 890V. Regarding the SM capacitances for MMC, in [47] it is suggested the maximum energy storage requirement of 40 kJ/MVA, which corresponds to a energy storage of $E_{nom} = 280kJ$. Therefore, the SM capacitance is given by [47]:

$$C = \frac{2E_{nom}}{9Nv_{sm}^2} = 13mF. \quad (1)$$

Regarding arm inductances, the per unit (pu) values for grid connected converters typically are limited in the range of 0.3 pu [48]. This work employs $L_{arm} = 0.15pu$, in order to reduce the high order harmonics in circulating current. Therefore, $L_{arm} = 0.21mH$.

C. DFR of Power Modules

Industrial motor drive applications works in most cases with a lifetime of 10–20 year, with a reduced proportion having a lifetime of 20–30 years, where the most fragile link is the power semiconductor devices [1]. In this way, the DFR is applied to ensure a minimum lifetime of 25 years during the IGBT power modules design. The three proposed solutions are analyzed: NPC, FT-ANPC and TSBC-MMC.

The first step to select the IGBT power module is based on the system parameters. For the NPC and FT-ANPC converter, the sizing is to withstand half of the dc-link voltage, while for the TSBC-MMC, it is performed considering a half of the SM nominal voltage. The dc-link voltage is $5.6kV$, while the SM nominal voltage is $890V$. Then, medium voltage power devices ($3300V$) for NPC and FT-ANPC, and low voltage power devices ($1700V$) for TSBC-MMC are selected. In terms of switching frequency, NPC and FT-ANPC converters employs 720 Hz while TSBC-MMC is switched in 525 Hz .

The current capacity of power devices is analyzed through the DFR approach, whose flowchart is exhibited in Figure 1. The selected converter is simulated on Plects with the rolling mill mission profile shown in Figure 3. The current and voltage are used to extract the losses of the selected power devices, that feed the thermal model. The ambient temperature is considered $40\text{ }^\circ\text{C}$. The rainflow algorithm is used to characterize the thermal cycling, provided by the thermal model. Finally, the ABB Hi-Pak IGBT power module lifetime model is used to estimate the B_{10} lifetime, which is the number of cycles where 10% of power modules fail [49]. If the expected lifetime is not achieved, the process is repeated, considering power devices with higher current capacity. When the system is working at the edge of the technology, power modules are inserted in parallel.

For the NPC converter, the required lifetime is ensured with two $5SNA1500E330305$ Hi-Pak power modules ($3300V/1500A$) in parallel. The IGBT junction temperature over a day for the back-to-back converter are shown in Figure 6 for both motor and grid side converters. Only the most stressed devices are show. For motor side converter, the most stressed device is the IGBT S1, which reaches a junction temperature of $79.1\text{ }^\circ\text{C}$. For grid side converter, the most stressed device is the IGBT S2, which reaches a junction temperature of $95.3\text{ }^\circ\text{C}$.

The FT-ANPC converter is capable of working in ANPC mode, equaling the losses and reducing the highest temperature. Furthermore, their thermal degradation management can prolong the power modules lifetime by about 250% [50]. As can be seen in Figure 7, the temperatures at the most stressed devices is considerably reduced to values smaller than $70\text{ }^\circ\text{C}$. Thereby, power modules with a reduced current capacity can be used, reducing the cost without extrapolating the lifetime limits.

The TSBC-MMC converter works at a reduced switching frequency and with low voltage power devices. As a consequence, the power losses is highly reduced, and this

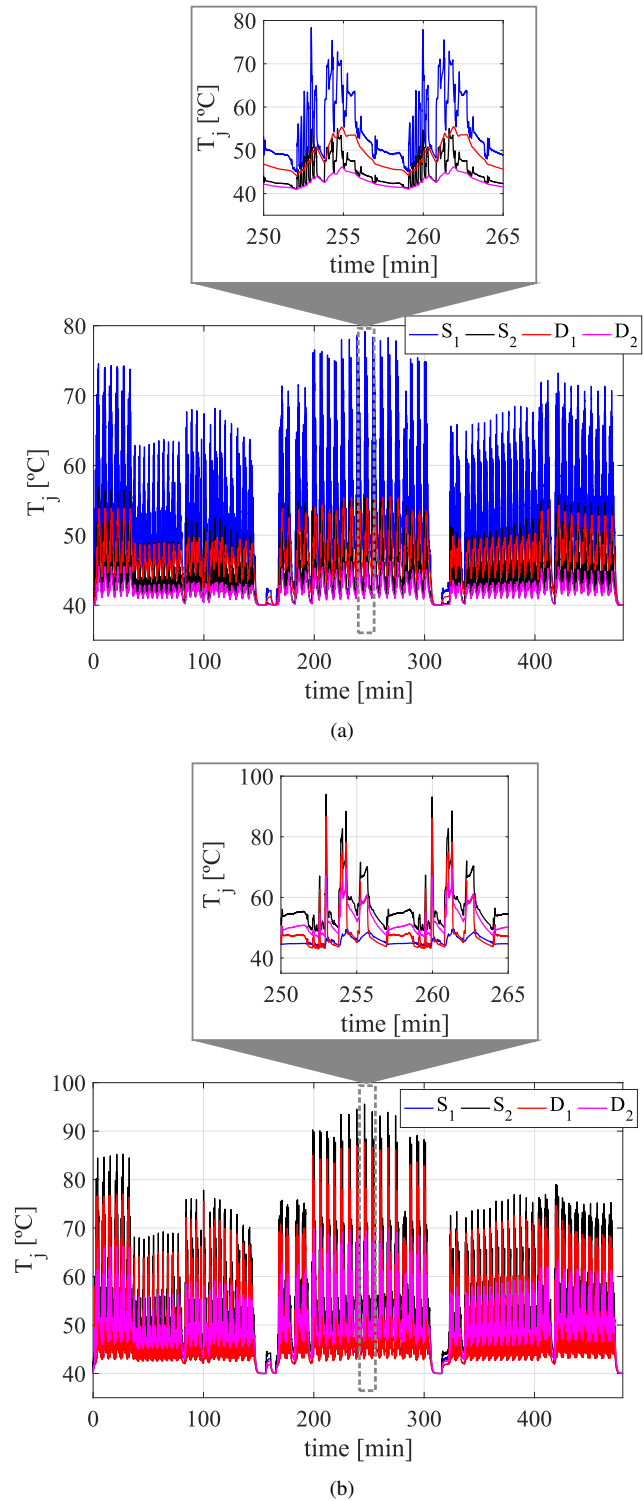
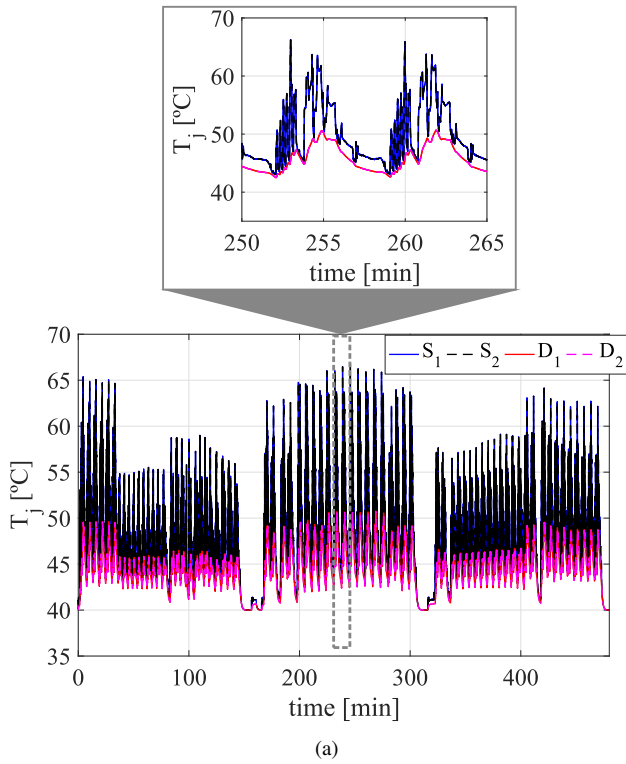
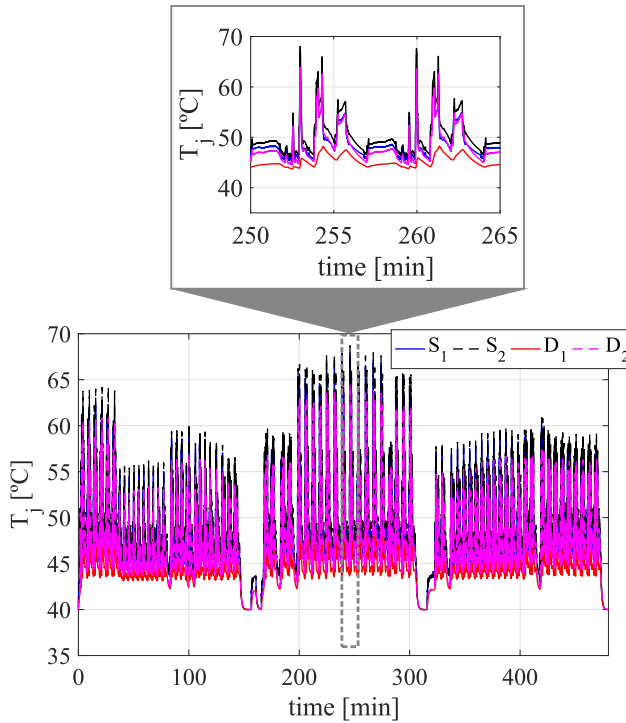


Fig. 6. Power devices junction temperatures of back-to-back NPC converter: (a) Motor side converter; (b) Grid side converter.

converter can ensure the required lifetime without parallelism. As can be seen in figure 8, the junction temperatures at the SMs is relatively low with $1700V/1600A$ power modules.



(a)



(b)

Fig. 7. Power devices junction temperatures of back-to-back FT-ANPC converter: (a) Motor side converter; (b) Grid side converter.

D. Losses and Cost Analysis

The comparison of the converter losses, following the mission profile is presented in Figure 9. The values are shown

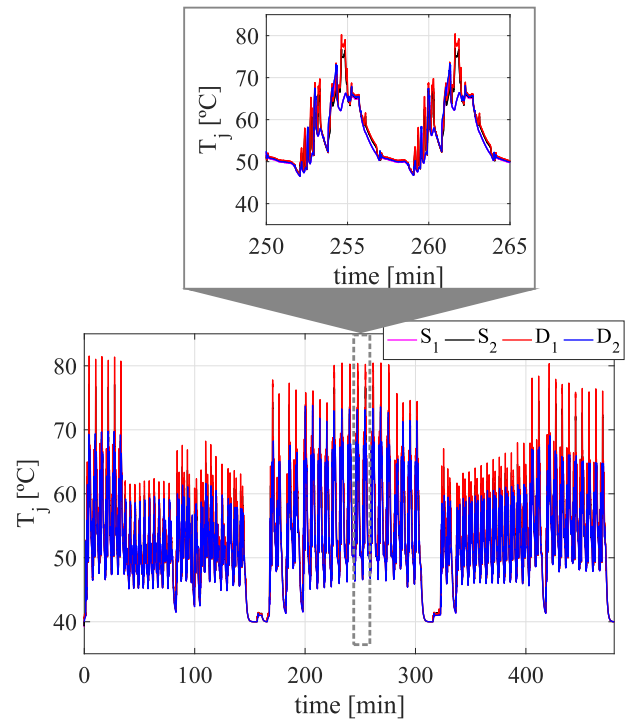


Fig. 8. Power devices junction temperatures of the TSBC-MMC.

in pu, considering a base value of 7 MVA. As observed, the losses are smaller than 0.013 pu for all operation conditions. TSBC-MMC topology present smaller losses while FT-ANPC can have larger or smaller losses depending of the operating conditions.

The total power consumption of the power devices is evaluated considering the losses profile shown in Figure 9. The obtained energy losses are 77.57 kWh, 85.73 kWh and 60.80 kWh for the NPC, FT-ANPC and TSBC-MMC, respectively. As observed, the TSBC-MMC presents smaller consumption due to its lower switching frequency and the inherent lower losses of low voltage power modules.

In figure 2, it is possible to observe that the system is composed by two back-to-back converters. Since each structure is composed by 2 back-to-back converters, then 4 NPCs are necessary. The overall cost of the solutions is directly related to the redundancy strategies employed. For the NPC converter, it is considered a back-to-back backup converter, which is a common practice in industry [1]. In this way, are necessary 6 NPC converters, totaling 144 IGBT power modules. The TSBC-MMC is designed with a redundancy factor of 10%, and no backup is necessary. Additionally, no redundancy is required for the FT-ANPC converter, due to its inherent fault tolerant capability.

The initial cost is based on the number of components required and the price per part number. These estimates are only indicative and the real system costs may vary depending upon a variety of factors such as civil and engineering costs which cannot be evaluated [11]. The system specification,

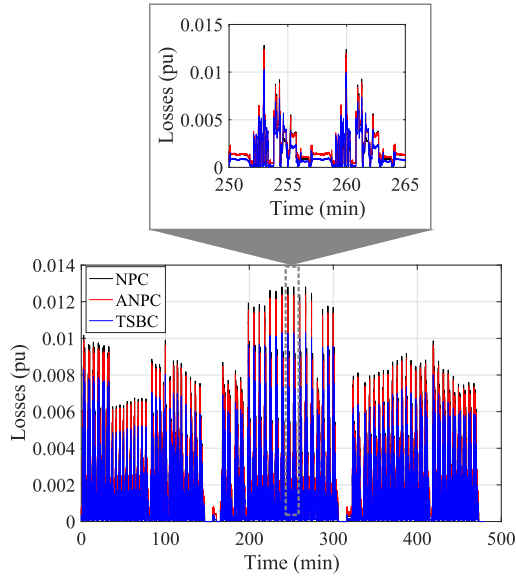


Fig. 9. Comparison of NPC, FT-ANPC and TSBC-MMC converters power losses considering the mission profile.

considering each topology with its redundancy strategies, are shown in Table II.

TABLE II
SPECIFICATIONS OF THE CONVERTERS.

Components	NPC	FT-ANPC	TSBC-MMC
IGBT modules	144	192	504
SM Capacitor kJ	282.24	188.16	616
Gate driver unit	144	192	504
Current sensor	18	12	30
Voltage sensor	12	8	66
Heatsink units	144	192	504
Mechanical Switch	-	6	63

The cost of the semiconductor devices, controls, cabinets is considered as 3.5 \$/kVA of the installed switching power. The switching power P_s is given by [10]:

$$P_s = N_{semi} V_{block} I_{rated}, \quad (2)$$

where N_{semi} is the number of semiconductors, V_{block} is the rated blocking voltage of the devices and I_{rated} is the rated device current. Additionally, the considered cost for the capacitors is 150 \$/kJ [10].

Table III shows the estimated converter costs. As observed, the capacitors represents a small amount of the total cost (smaller than 1.6 % of total cost). For the presented case, the FT-ANPC solution presents is 1.3 times more expensive than standard solution. For TSBC-MMC topology, the converter price is 3.7 times more expensive. The larger number of switches considerably increase the cost of the TSBC-MMC.

IV. DECISION MAKING

A system field failure of motor drive applications may be higher than a single system cost, which includes replacement free of charge, travel cost maintenance personnel, and penalty

TABLE III
ESTIMATED COST OF THE INVERTERS.

Components	NPC	FT-ANPC	TSBC-MMC
Power Electronics	2,494,800 \$	3,326,400 \$	9,313,920 \$
Capacitors	42,336 \$	28,224 \$	92,400 \$
Total	2,537,136 \$	3,354,624 \$	9,406,320 \$

charges [1]. This fact underscores the importance of a thorough analysis during the evaluation and selection of a converter for critical applications. The decision-making of the methodology can be based on the relationship between investment capacity and metrics of reliability.

This work presents three solutions, each one with its particularities. The NPC converter with backup can overcome up to two failure situation in any element, independent of the failure mechanism. Maintenance time is required during the converter exchange. The option for FT-ANPC converter is 30% more expensive. However, each converter can survive up to four open-circuit failure situation in its power devices, totaling 16 specific failure events.

The TSBC-MMC, is 3.7 time more expensive, yet it has greater flexibility of fault tolerance. It is able to overcome 9 failure events, independent of the mechanism and element. Hence, the failure history can be another important parameter during the decision-making process.

Additionally, the energy losses for TSBC-MMC are smaller, which results in smaller operational costs. Depending of the value of energy tariffs, the converter can become cheaper during its lifetime. Nevertheless, this detailed economic analysis is out the scope of this work.

V. CONCLUSIONS

This work proposes a methodology for design and selection of high reliability power converters in MCIA. A rolling mill system from a big steel industry in southeastern Brazil is adopted as case study. This study is detailed step-by-step in order to become possible the understanding and repeating. In such conditions, design and field engineers can employ this methodology to design or select a high reliability converter for a specific application.

Two high reliability alternatives were proposed to substitute the standard NPC solution: The FT-ANPC and the TSBC-MMC. The importance of DFR in mission critical applications was once again highlighted. The evaluation of IGBTs power modules considering the real mission profile was demonstrated. The cost and losses analysis were chosen as a final selection criteria. Two high reliability alternatives were proposed to substitute the standard NPC solution: The FT-ANPC and the TSBC-MMC. The importance of DFR in mission critical applications was once again highlighted. The evaluation of IGBTs power modules considering the real mission profile was demonstrated. The cost and losses analysis were chosen as a final selection criteria.

The decision-making section was developed to highlight some important points during the system choice and design. It is known that there are more complex decision-making

processes and specific issues to be addressed by the experts from each industry. This goes beyond the scope of this work. Nevertheless, the proposed methodology certainly can be combined to any refined decision-making process.

ACKNOWLEDGMENT

The authors would like to thank the financial support from CEFET-MG and the Brazilian federal government agencies CAPES and CNPq (research grant no. 459459/2014-7), and the Minas Gerais state government agency FAPEMIG.

REFERENCES

- [1] S. Yang, A. Bryant, P. Mawby, D. Xiang, L. Ran, and P. Tavner, "An industry-based survey of reliability in power electronic converters," *IEEE Transactions on Industry Applications*, vol. 47, no. 3, pp. 1441–1451, May 2011.
- [2] T. J. Hesla, "Electrification of a major steel mill part 5: Scherbius and kraemer drives [history]," *IEEE Industry Applications Magazine*, vol. 13, no. 4, pp. 8–11, July 2007.
- [3] S. Madhusoodhanan, K. Mainali, A. Tripathi, K. Vechalapu, and S. Bhattacharya, "Medium voltage (2.3 kv) high frequency three-phase two-level converter design and demonstration using 10 kv sic mosfets for high speed motor drive applications," in *2016 IEEE Applied Power Electronics Conference and Exposition (APEC)*, March 2016, pp. 1497–1504.
- [4] E. Cengelci, P. N. Enjeti, and J. W. Gray, "A new modular motor-modular inverter concept for medium-voltage adjustable-speed-drive systems," *IEEE Transactions on Industry Applications*, vol. 36, no. 3, pp. 786–796, May 2000.
- [5] J. Dai, S. W. Nam, M. Pande, and G. Esmaeili, "Medium-voltage current-source converter drives for marine propulsion system using a dual-winding synchronous machine," *IEEE Transactions on Industry Applications*, vol. 50, no. 6, pp. 3971–3976, Nov 2014.
- [6] D. Krug, M. Malinowski, and S. Bernet, "Design and comparison of medium voltage multi-level converters for industry applications," in *Conference Record of the 2004 IEEE Industry Applications Conference, 2004. 39th IAS Annual Meeting.*, vol. 2, 2004, pp. 781–790 vol.2.
- [7] T. Bruckner, S. Bernet, and H. Guldner, "The active npc converter and its loss-balancing control," *IEEE Transactions on Industrial Electronics*, vol. 52, no. 3, pp. 855–868, June 2005.
- [8] D. Andler, R. Álvarez, S. Bernet, and J. Rodríguez, "Switching loss analysis of 4.5-kv;5.5-ka igcets within a 3l-anpc phase leg prototype," *IEEE Transactions on Industry Applications*, vol. 50, no. 1, pp. 584–592, Jan 2014.
- [9] K. Fujii, U. Schwarzer, and R. W. D. Doncker, "Comparison of hard-switched multi-level inverter topologies for statcom by loss-implemented simulation and cost estimation," in *36th PESC*, June 2005, pp. 340–346.
- [10] S. P. Engel, M. Stieneker, N. Soltau, S. Rabiee, H. Stagge, and R. W. D. Doncker, "Comparison of the modular multilevel dc converter and the dual-active bridge converter for power conversion in hvdc and mvdc grids," *IEEE Transactions on Power Electronics*, vol. 30, no. 1, pp. 124–137, Jan 2015.
- [11] H. A. B. Siddique, A. R. Lakshminarasimhan, C. I. Odeh, and R. W. D. Doncker, "Comparison of modular multilevel and neutral-point-clamped converters for medium-voltage grid-connected applications," in *2016 IEEE International Conference on Renewable Energy Research and Applications (ICRERA)*, Nov 2016, pp. 297–304.
- [12] A. Anurag, Y. Yang, and F. Blaabjerg, "Reliability analysis of single-phase pv inverters with reactive power injection at night considering mission profiles," in *2015 IEEE Energy Conversion Congress and Exposition (ECCE)*, Sept 2015, pp. 2132–2139.
- [13] Y. Yang, A. Sangwongwanich, and F. Blaabjerg, "Design for reliability of power electronics for grid-connected photovoltaic systems," *CPSS Transactions on Power Electronics and Applications*, vol. 1, no. 1, pp. 92–103, Dec 2016.
- [14] A. Sangwongwanich, Y. Yang, D. Sera, and F. Blaabjerg, "Lifetime evaluation of pv inverters considering panel degradation rates and installation sites," in *2017 IEEE Applied Power Electronics Conference and Exposition (APEC)*, March 2017, pp. 2845–2852.
- [15] Y. Yang, K. Ma, H. Wang, and F. Blaabjerg, "Mission profile translation to capacitor stresses in grid-connected photovoltaic systems," in *2014 IEEE Energy Conversion Congress and Exposition (ECCE)*, Sept 2014, pp. 5479–5486.
- [16] A. Isidori, F. M. Rossi, F. Blaabjerg, and K. Ma, "Thermal loading and reliability of 10-mw multilevel wind power converter at different wind roughness classes," *IEEE Transactions on Industry Applications*, vol. 50, no. 1, pp. 484–494, Jan 2014.
- [17] H. Liu, K. Ma, Z. Qin, P. C. Loh, and F. Blaabjerg, "Lifetime estimation of mmc for offshore wind power hvdc application," *IEEE Journal of Emerging and Selected Topics in Power Electronics*, vol. 4, no. 2, pp. 504–511, June 2016.
- [18] K. Ma, M. Liserre, and F. Blaabjerg, "Reactive power influence on the thermal cycling of multi-mw wind power inverter," *IEEE Transactions on Industry Applications*, vol. 49, no. 2, pp. 922–930, March 2013.
- [19] K. Ma, M. Liserre, F. Blaabjerg, and T. Kerekes, "Thermal loading and lifetime estimation for power device considering mission profiles in wind power converter," *IEEE Transactions on Power Electronics*, vol. 30, no. 2, pp. 590–602, Feb 2015.
- [20] M. Andresen, K. Ma, G. D. Carne, G. Buticchi, F. Blaabjerg, and M. Liserre, "Thermal stress analysis of medium-voltage converters for smart transformers," *IEEE Transactions on Power Electronics*, vol. 32, no. 6, pp. 4753–4765, June 2017.
- [21] M. Andresen, V. Raveendran, G. Buticchi, and M. Liserre, "Lifetime-based power routing in parallel converters for smart transformer application," *IEEE Transactions on Industrial Electronics*, vol. 65, no. 2, pp. 1675–1684, Feb 2018.
- [22] R. Zhu, H. Jedtberg, and M. Liserre, "Voltage control strategies of smart transformer considering dc capacitor lifetime," in *IECON 2017 - 43rd Annual Conference of the IEEE Industrial Electronics Society*, Oct 2017, pp. 4278–4283.
- [23] V. N. Ferreira, G. A. Mendonca, A. V. Rocha, R. S. Resende, and B. J. C. Filho, "Mission critical analysis and design of igbt-based power converters applied to mine hoist systems," *IEEE Transactions on Industry Applications*, vol. PP, no. 99, pp. 1–1, 2017.
- [24] A. V. Rocha, S. M. Silva, I. A. Pires, A. A. P. Machado, F. V. Amaral, V. N. Ferreira, H. de Paula, and B. J. C. Filho, "A new fault-tolerant realization of the active three-level npc converter," in *2014 IEEE Energy Conversion Congress and Exposition (ECCE)*, Sept 2014, pp. 3483–3490.
- [25] Y. Okazaki, W. Kawamura, M. Hagiwara, H. Akagi, T. Ishida, M. Tsukakoshi, and R. Nakamura, "Experimental comparisons between modular multilevel dsc inverters and tsbc converters for medium-voltage motor drives," *IEEE Transactions on Power Electronics*, vol. 32, no. 3, pp. 1805–1817, March 2017.
- [26] W. Kawamura, M. Hagiwara, and H. Akagi, "Control and experiment of a modular multilevel cascade converter based on triple-star bridge cells," *IEEE Transactions on Industry Applications*, vol. 50, no. 5, pp. 3536–3548, Sept 2014.
- [27] F. Kammerer, J. Kolb, and M. Braun, "A novel cascaded vector control scheme for the modular multilevel matrix converter," in *IECON 2011 - 37th Annual Conference of the IEEE Industrial Electronics Society*, Nov 2011, pp. 1097–1102.
- [28] V. de Nazareth Ferreira, A. F. Cupertino, H. A. Pereira, A. V. Rocha, S. I. Seleme, and B. de Jesus Cardoso Filho, "Design of high-reliable converters for medium-voltage rolling mills systems," in *2017 IEEE Industry Applications Society Annual Meeting*, Oct 2017, pp. 1–9.
- [29] Q. Tu and Z. Xu, "Power losses evaluation for modular multilevel converter with junction temperature feedback," in *IEEE Power and Energy Society General Meeting*, July 2011, pp. 1–7.
- [30] K. Ma, N. He, M. Liserre, and F. Blaabjerg, "Frequency-domain thermal modeling and characterization of power semiconductor devices," *IEEE Transactions on Power Electronics*, vol. 31, no. 10, pp. 7183–7193, Oct 2016.
- [31] V. N. Ferreira, G. A. Mendonça, A. V. Rocha, R. S. Resende, and B. J. C. Filho, "Proactive fault-tolerant igbt-based power converters for mission critical applications in mw range," in *Applied Power Electronics Conference*, 2017.
- [32] W. Kawamura, M. Hagiwara, H. Akagi, M. Tsukakoshi, R. Nakamura, and S. Kodama, "Ac-inductors design for a modular multilevel tsbc converter, and performance of a low-speed high-torque motor drive using the converter," *IEEE Transactions on Industry Applications*, vol. PP, no. 99, pp. 1–1, 2017.

- [33] D. Andler, R. Álvarez, S. Bernet, and J. Rodríguez, "Experimental investigation of the commutations of a 3l-anpc phase leg using 4.5-kv;5.5-ka igcts," *IEEE Transactions on Industrial Electronics*, vol. 60, no. 11, pp. 4820–4830, Nov 2013.
- [34] H. W. van der Broeck, H. C. Skudelny, and G. V. Stanke, "Analysis and realization of a pulsewidth modulator based on voltage space vectors," *IEEE Transactions on Industry Applications*, vol. 24, no. 1, pp. 142–150, Jan 1988.
- [35] T. Bruckner, S. Bernet, and P. K. Steimer, "Feedforward loss control of three-level active npc converters," *IEEE Transactions on Industry Applications*, vol. 43, no. 6, pp. 1588–1596, Nov 2007.
- [36] D. W. Novotny and T. Lipo, *Vector Control and Dynamics of ac Drives*. Clarendon Press, 1996.
- [37] M. Liserre, A. Dell'Aquila, and F. Blaabjerg, "An overview of three-phase voltage source active rectifiers interfacing the utility," in *2003 IEEE Bologna Power Tech Conference Proceedings*, vol. 3, June 2003, pp. 8 pp. Vol.3–.
- [38] F. Z. Peng, J.-S. Lai, J. W. McKeever, and J. VanCoevering, "A multilevel voltage-source inverter with separate dc sources for static var generation," *IEEE Transactions on Industry Applications*, vol. 32, no. 5, pp. 1130–1138, Sep 1996.
- [39] B. Gemmel, J. Dorn, D. Retzmann, and D. Soerangr, "Prospects of multilevel vsc technologies for power transmission," in *2008 IEEE/PES Transmission and Distribution Conference and Exposition*, April 2008, pp. 1–16.
- [40] G. T. Son, H. J. Lee, T. S. Nam, Y. H. Chung, U. H. Lee, S. T. Baek, K. Hur, and J. W. Park, "Design and control of a modular multilevel hvdc converter with redundant power modules for noninterruptible energy transfer," *IEEE Transactions on Power Delivery*, vol. 27, no. 3, pp. 1611–1619, July 2012.
- [41] M. Davies, M. Dommaschk, J. Dorn, J. Lang, D. Retzmann, and D. Soerangr, "Hvdc plus - basics and principle of operation," SIEMENS, Tech. Rep., 2017.
- [42] G. S. Konstantinou, M. Ciobotaru, and V. G. Agelidis, "Effect of redundant sub-module utilization on modular multilevel converters," in *2012 IEEE International Conference on Industrial Technology*, March 2012, pp. 815–820.
- [43] N. Ahmed, L. Ångquist, A. Antonopoulos, L. Harnefors, S. Norrga, and H. P. Nee, "Performance of the modular multilevel converter with redundant submodules," in *IECON 2015 - 41st Annual Conference of the IEEE Industrial Electronics Society*, Nov 2015, pp. 003 922–003 927.
- [44] B. Li, Y. Zhang, R. Yang, R. Xu, D. Xu, and W. Wang, "Seamless transition control for modular multilevel converters when inserting a cold-reserve redundant submodule," *IEEE Transactions on Power Electronics*, vol. 30, no. 8, pp. 4052–4057, Aug 2015.
- [45] P. Hu, D. Jiang, Y. Zhou, Y. Liang, J. Guo, and Z. Lin, "Energy-balancing control strategy for modular multilevel converters under submodule fault conditions," *IEEE Transactions on Power Electronics*, vol. 29, no. 9, pp. 5021–5030, Sept 2014.
- [46] Y. Okazaki, H. Matsui, M. Hagiwara, and H. Akagi, "Research trends of modular multilevel cascade inverter (mmci-dscc)-based medium-voltage motor drives in a low-speed range," in *2014 International Power Electronics Conference (IPEC-Hiroshima 2014 - ECCE ASIA)*, May 2014, pp. 1586–1593.
- [47] K. Ilves, L. Bessegato, and S. Norrga, "Comparison of cascaded multilevel converter topologies for ac/ac conversion," in *2014 International Power Electronics Conference (IPEC-Hiroshima 2014 - ECCE ASIA)*, May 2014, pp. 1087–1094.
- [48] K. Sharifabadi, L. Harnefors, H. Nee, S. Norrga, and R. Teodorescu, *Design, Control and Application of Modular Multilevel Converters for HVDC Transmission Systems*. John Wiley & Sons, 2016.
- [49] ABB Application note., "Load-cycling Capability of Hi-Pak IGBT Modules."
- [50] V. N. Ferreira, A. V. Rocha, and B. J. C. Filho, "Thermal degradation management in a fault-tolerant active npc converter," in *2015 IEEE 13th Brazilian Power Electronics Conference and 1st Southern Power Electronics Conference (COBEP/SPEC)*, Nov 2015, pp. 1–6.